

# One-Step Direct Transfer of Pristine Single-Walled Carbon Nanotubes for Functional Nanoelectronics

Chung Chiang Wu, Chang Hua Liu, and Zhaohui Zhong\*

Department of Electrical Engineering and Computer Science, University of Michigan, Ann Arbor, Michigan 48109

**ABSTRACT** We report a one-step direct transfer technique for the fabrication of functional nanoelectronic devices using pristine single-walled carbon nanotubes (SWNTs). Suspended SWNTs grown by the chemical vapor deposition (CVD) method are aligned and directly transferred onto prepatterned device electrodes at ambient temperature. Using this technique, we successfully fabricated SWNT electromechanical resonators with gate-tunable resonance frequencies. A fully suspended SWNT p–n diode has also been demonstrated with the diode ideality factor equal to 1. Our method eliminates the organic residues on SWNTs resulting from conventional lithography and solution processing. The results open up opportunities for the fundamental study of electron transport physics in ultraclean SWNTs and for room temperature fabrication of novel functional devices based on pristine SWNTs.

**KEYWORDS** Carbon nanotube, direct transfer, nanoelectromechanical resonator, p–n diode

Single-walled carbon nanotubes (SWNTs) are one-dimensional nanostructures with remarkable electrical, mechanical, and optical properties.<sup>1,2</sup> They are ideal platform for understanding low dimensional physics as well as exploring novel device applications due to quantum size effect.<sup>3</sup> The high carrier mobilities of SWNTs lead to high-performance nanoelectronic devices and circuits,<sup>4–7</sup> which have the potential of operating at terahertz frequencies.<sup>8,9</sup> In addition, SWNTs have very low mass density and Young's modulus of  $\sim 1$  TPa,<sup>10</sup> making them ideal building blocks for nanoelectromechanical systems (NEMS).<sup>11–13</sup> Suspended nanotubes have been demonstrated as NEMS resonators,<sup>14–17</sup> with the potential application as ultrasensitive mass sensors.<sup>18,19</sup> Furthermore, semiconducting SWNTs are direct-band-gap materials capable of efficient absorption and emission of photons.<sup>20–24</sup> SWNT p–n diodes have been fabricated both on substrate and partially suspended,<sup>25–27</sup> with diode ideality factors close to unity. Light-emitting diodes (LEDs) and photodetectors have been demonstrated using SWNTs.<sup>28–30</sup> Recent study also showed extremely efficient multiple electron–hole pairs generation in SWNTs, suggesting potential photovoltaic applications utilizing SWNTs as the light absorber.<sup>31</sup>

Conventionally, SWNT nanoelectronic and nanophotonic devices are fabricated through either postgrowth fabrication or postfabrication growth approaches.<sup>1,32,33</sup> For the postgrowth fabrication method, SWNTs are first placed onto a device substrate by either direct chemical vapor deposition (CVD) growth or indirect solution process. Lithography is then carried out to define the functional devices. This

method is widely adopted, yet SWNTs are inevitably contaminated by organic residues resulting from the lithography and solution processing. To eliminate contaminations, a postfabrication growth method is developed to avoid solution processing. Lithography is carried out first to define electrical contacts made out of high melting temperature metals (such as platinum). SWNTs are subsequently grown directly on top of the electrodes by CVD method. This technique results in ultraclean SWNT devices, but the high growth temperature ( $\sim 900$  °C) prohibits its wide applications. More recently, SWNTs grown on substrate were also shown to be transferred onto electrodes by stamping.<sup>34,35</sup> However, potential contamination and damages to SWNTs can come from the stamping process, and the registry of SWNTs to the electrodes is entirely random.

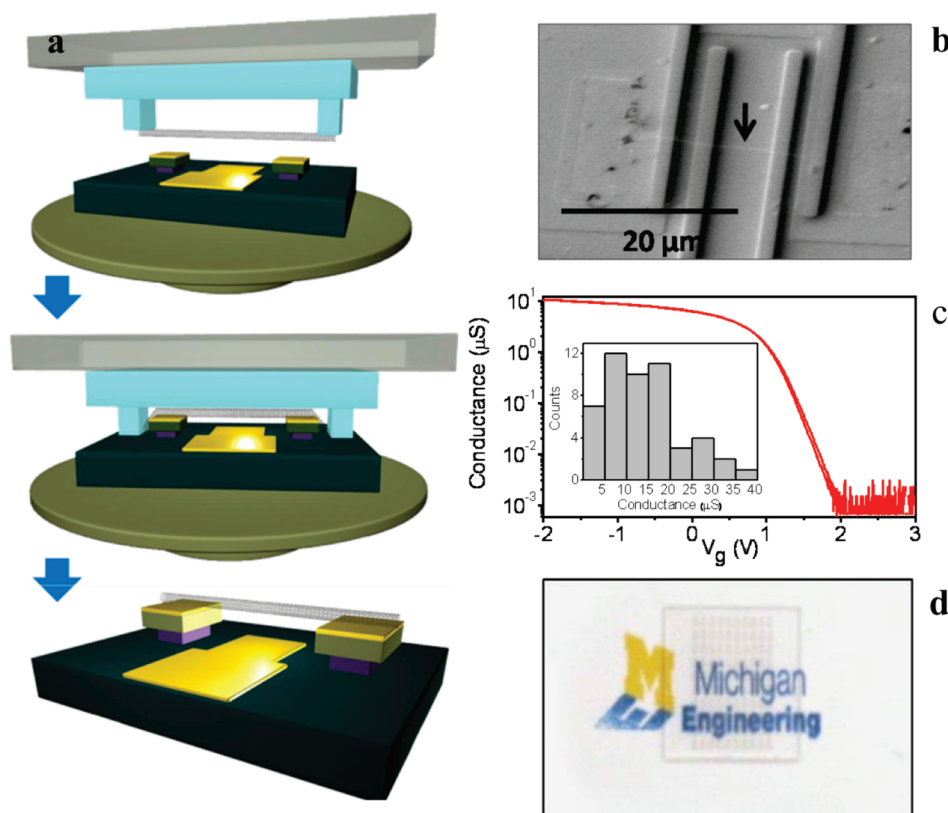
Despite this recent progress, low temperature controlled fabrication of pristine SWNT devices is still a challenging yet important task. To this end, we successfully develop a one-step direct transfer technique to fabricate functional nanoelectronic devices from suspended CVD grown SWNTs. Nanotubes, grown on a separate substrate, are aligned and directly transferred to prefabricated electrodes on a device substrate. Importantly, the process is carried out at ambient condition and without contamination from solution processing. To prove the reliability and feasibility of our one-step direct transfer technique, nanoelectronic devices including NEMS resonators and fully suspended SWNT p–n diodes are demonstrated. The technique is particularly attractive for exploring fundamental physics in ultraclean SWNTs and for novel applications, such as flexible nanoelectronics and nanoelectronic sensors, where room temperature fabrication of pristine SWNT devices is desirable.

Figure 1a illustrates the procedure of the one-step direct transfer technique. Suspended SWNTs are grown across

\* Corresponding author, zzhong@umich.edu.

Received for review: 12/24/2009

Published on Web: 00/00/0000



**FIGURE 1.** One-step direct transfer of pristine SWNTs for functional devices. (a) Schematic of direct transfer procedure. A suspended SWNT grown on a quartz substrate is mounted upside-down on a blank mask, and a device substrate with prefabricated electrodes is placed on the stage of the contact aligner (top panel). The quartz substrate is aligned to the device substrate and subsequently brought into contact by lifting the stage (middle panel). SWNTs are cut off at the contact points and span across the electrodes (bottom panel). (b) SEM image of a typical device fabricated using direct transfer method. The arrow indicates the position of nanotube. Scale bar: 20  $\mu\text{m}$ . (c) Conductance vs gate voltage curve for a typical suspended SWNT transistor. The inset shows the conductance histogram of 50 devices. (d) Optical image of SWNT devices on transparent glass substrate. Die with size 1 cm  $\times$  1 cm is placed on top of a “Michigan Engineering” logo.

pillars on transparent quartz substrate using a high-temperature CVD method,<sup>36</sup> while the device substrate containing predesigned electrodes, such as source, drain, and gate electrodes for a field effect transistor (FET), is fabricated at room temperature using a conventional lithography technique (see Supporting Information). Contact aligner (Karl Suss MJB-3) is then used to facilitate the one-step direct transfer. The quartz substrate is mounted upside-down on a blank glass mask, while the device substrate is placed on the sample stage of the aligner (Figure 1a, top panel). By use of matching alignment keys, the quartz substrate is aligned to the device substrate and subsequently brought into contact by lifting the stage (Figure 1a, middle panel). Because the spacing of the pillars is designed to be wider than the electrode spacing, SWNTs are cut off at the contact points between the pillars and the substrate and span across the electrodes (Figure 1a, lower panel). As a result, functional SWNT nanoelectronics are readily formed without the need of further lithography, eliminating potential contamination on the nanotubes. Figure 1b shows the scanning electron microscope (SEM) image of a typical device fabricated using the direct transfer method, in which a single nanotube spans across four prepatterned metal electrodes.

The electrical contact between a nanotube and metal electrode resulting from direct transfer is evaluated using a suspended SWNT FET configuration (Figure 1a). Nanotube channel lengths are designed to be 1–3  $\mu\text{m}$ , while Au and Pd are explored as bottom-contact metals. Figure 1c shows a conductance vs gate voltage curve for a typical nanotube transistor. Classic transfer characteristics of a p-channel FET is observed, with ON state conductance of 12  $\mu\text{S}$  and ON/OFF ratio larger than 4 orders of magnitude.<sup>37</sup> The device also exhibits negligible hysteresis, indicating that the nanotube is indeed suspended in air. Similar results are obtained on 50 devices, and histogram suggests an average ON state conductance of  $\sim 12 \mu\text{S}$  (Figure 1c, inset). These results are comparable with top-contacted nanotube transistors, confirming that our simple on-step direct transfer technique results in similar contact resistance as conventional fabrication technique. In addition, thermal annealing is helpful for reducing the device contact resistance but not necessary for freshly deposited metals.<sup>38</sup>

We further investigate the SWNT device yield from one-step direct transfer technique. SEM is used to first identify 14 pairs of pillars on quartz substrate which have one or a few nanotubes suspended across. After transfer, electrical

measurements confirm that 13 out of 14 devices are successfully fabricated, corresponding to  $\sim 92\%$  transfer yield. 100% transfer is possible by modifying our setup to allow precise control of contact force. The overall yield is thus dictated by the growth yield of nanotubes suspended across the pillars, which can be controlled statistically by the pillar dimensions and growth condition. In this work, we tune our growth condition to have on-average a single nanotube within an individual device, which results in an overall device yield of  $\sim 20\text{--}40\%$ .

Our technique can be widely adopted on different types of substrates since the transfer process is carried out under ambient condition. In addition to the suspended devices, we have also fabricated nonsuspended SWNT FET devices on substrate with high- $\kappa$  dielectrics (data not shown). SWNT devices on a transparent glass substrate have also been demonstrated through one-step direct transfer (Figure 1d). Moreover, we believe the technique can be readily applied onto a plastic substrate for flexible nanoelectronics and nanophotonics.

To demonstrate the versatility of our technique, we first fabricate SWNT NEMS resonators by one-step direct transfer. The devices have similar geometry as shown in Figure 1a, with nanotube length of  $1\text{--}3\ \mu\text{m}$  and nanotube/bottom-gate separation of  $1\ \mu\text{m}$ . Alternating current driving voltage between the nanotube and the bottom-gate electrode actuates the resonator through electrostatic interaction, and resonance frequency is detected using a single-source mixing technique described in the literature.<sup>14,39</sup> Figure 2 shows the electromechanical responses of a typical SWNT resonator with channel length of  $3\ \mu\text{m}$ . A frequency-dependent mixing current,  $I_{\text{mix}}$ , sweep at  $V_g = 3\ \text{V}$  between 20 and 30 MHz reveals a clear peak, corresponding to the guitar-string-like resonance mode of the doubly clamped nanotube resonator (Figure 2a, dots). Lorentzian fit (Figure 2a, line) yields resonance frequency,  $f = 26.1\ \text{MHz}$  with quality factor  $Q = 90$ .

We further investigate the frequency tuning of nanotube resonator by sweeping the bottom-gate voltage. In Figure 2b, mixing current (in color) is plotted as a function of driving frequency and gate voltage. Three resonance modes are clearly observed with strong gate dependence, corresponding to the in-plane and out-of-plan vibrational modes of the nanotube.<sup>14,15</sup> We further extract the resonance frequencies with respect to the gate voltages for all three modes and plot them in Figure 2c. Three types of gate dependence are observed, quadratic ( $f \sim V_g^2$ , in red), linear ( $f \sim V_g$ , in black), and sublinear ( $f \sim V_g^{0.7}$ , in green), which correspond to bending regime, catenary regime, and elastic regime, respectively. Increased tension due to increased gate voltage causes transition from the bending regime to the catenary regime, and eventually to the elastic regime, which is clearly visible for the second vibrational mode.

Similar results have been obtained on 16 other SWNT resonators, with quality factors ranging among 30–150 at

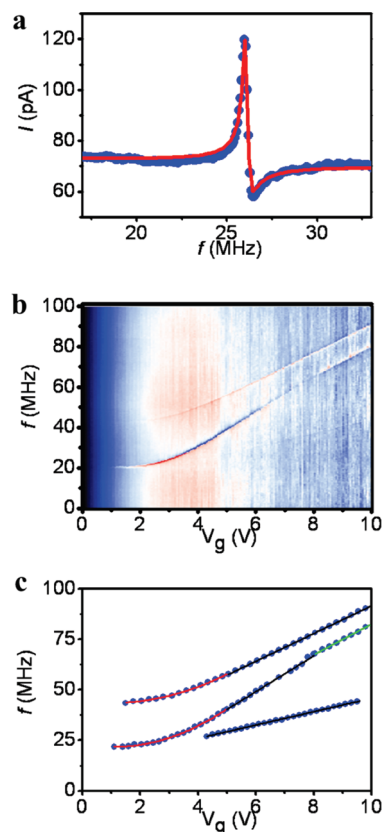


**FIGURE 2.** SWNT nanoelectromechanical resonators. (a) Mixing currents as a function of driving frequency between 20 and 30 MHz. Gate voltage  $V_g = 3\ \text{V}$ , ac driving voltage amplitude  $\delta V = 10\ \text{mV}$ . Dots are the experimental data, and the solid line is the Lorentzian fitting which yields  $f = 26.1\ \text{MHz}$  and quality factor  $Q = 90$ . (b) Mixing current (in color scale) is plotted as a function of driving frequency and gate voltage. Three vibrational resonances are clearly observed. (c) Resonance frequencies vs the gate for all three modes. The data are plotted in color, quadratic dependence ( $f \sim V_g^2$ ) in red, linear ( $f \sim V_g$ ) in black, and sublinear ( $f \sim V_g^{0.7}$ ) in green. All resonance measurements are done in a vacuum chamber at pressure below  $10^{-4}$  Torr.

room temperature, and resonance frequencies among 5–200 MHz. These results are comparable with previous devices made by conventional techniques, suggesting that our much simplified fabrication technique yields high quality nanotube resonators. In addition, multiple resonators can be fabricated on a single nanotube, opening up possibilities for investigating coupled 1D NEMS resonators in series.

The second type of functional nanoelectronic device we demonstrated using the one-step direct transfer technique is a fully suspended SWNT p–n diode. As shown in Figure 3a, a pristine SWNT is transferred and suspended across two split bottom gates, G1 and G2. The polarity of the two nanotube sections above the bottom gates is controlled by electrostatic doping through applying gate voltages, respectively.  $I$ – $V$  characteristics of a typical device are shown in Figure 3b. When gate voltages of  $V_{g1} = V_{g2} = -2\ \text{V}$  are applied, a linear  $I$ – $V$  is observed with resistance of  $300\ \text{k}\Omega$ . In this case, both sections are p-doped, and the device behaves as a resistor (Figure 3b, in blue). When the gate

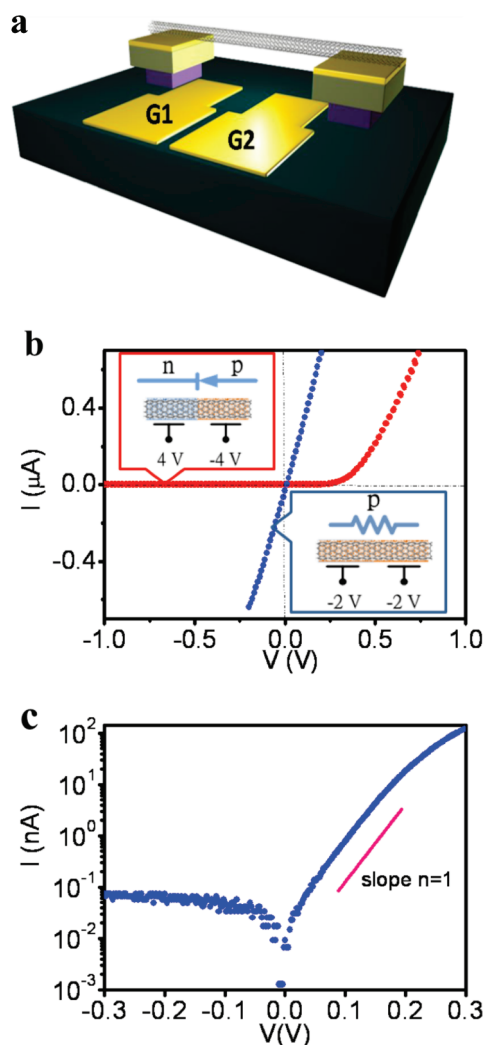


**FIGURE 3.** Fully suspended SWNT p–n diode. (a) Schematic of device geometry. G1 and G2 are two split gates for the electrostatic doping of nanotube to create a p–n junction. The separation between two gates is 1  $\mu\text{m}$ , and the width of each gate electrode is also 1  $\mu\text{m}$ . The separation between nanotube and gate electrode is 2  $\mu\text{m}$ . (b)  $I$ – $V$  characteristics of a suspended SWNT p–n diode. Linear behavior is observed when  $V_{g1} = V_{g2} = -2$  V (blue line); the rectification behavior is observed at  $V_{g1} = 4$  V and  $V_{g2} = -4$  V (red line). (c)  $I$ – $V$  plot in absolute magnitude of the current at gating voltages  $V_{g1} = -V_{g2} = 4$  V (blue dots). The red line corresponds to ideality factor  $n = 1$  in ideal diode equation.

voltages are changed to  $V_{g1} = 4$  V and  $V_{g2} = -4$  V, we obtain a rectified  $I$ – $V$  curve. Here positive  $V_{g1}$  n-dopes the nanotube section above G1 and negative  $V_{g2}$  p-dopes the nanotube section above G2, forming a p–n junction (Figure 3b, in red). Significantly, a log-scale  $I$ – $V$  plot (Figure 3c) reveals that the fully suspended SWNT p–n diode has an ideality factor of 1 and reversed saturation current of 45 pA at room temperature. These results point toward novel optoelectronic applications by exploiting the fully suspended nanotube ideal diodes.

In summary, we have reported a powerful yet simple one-step fabrication technique for SWNT devices. Using this

technique, we demonstrate the fabrication of nanotube electromechanical resonators and fully suspended SWNT ideal diodes. The technique can find wide applications for pristine nanotube electronic and photonic devices. It should also benefit the integration of a nanotube device onto a nonconventional substrate where device processing needs to be carried out at ambient conditions.

**Acknowledgment.** The authors thank Professor John Hart and Dr. Yongyi Zhang for assistance in nanotube synthesis. The work is supported by the startup fund provide by the University of Michigan. This work used the Lurie Nanofabrication Facility at University of Michigan, a member of the National Nanotechnology Infrastructure Network funded by the National Science Foundation.

**Supporting Information Available.** Details of synthesis of suspended carbon nanotubes and the process of prepatterned device electrodes. This material is available free of charge via the Internet at <http://pubs.acs.org>.

## REFERENCES AND NOTES

- (1) Dresselhaus, M. D.; Avouris, P., *Carbon Nanotubes: Synthesis, Structure Properties and Applications*; Springer-Verlag: Berlin, 2001.
- (2) Saito, R.; Dresselhaus, G.; Dresselhaus, M. S., *Physical Properties of Carbon Nanotubes*; Imperial College Press: London, 1998.
- (3) McEuen, P. L.; Park, J. Y. *MRS Bull.* **2004**, *29*, 272.
- (4) Zhou, X. J.; Park, J. Y.; Huang, S. M.; Liu, J.; McEuen, P. L. *Phys. Rev. Lett.* **2005**, *95*, 146805.
- (5) McEuen, P. L.; Fuhrer, M. S.; Park, H. K. *IEEE Trans. Nanotechnol.* **2002**, *1*, 78.
- (6) Avouris, P.; Chen, Z. H.; Perebeinos, V. *Nat. Nanotechnol.* **2007**, *2*, 605.
- (7) Dai, H. J.; Javey, A.; Pop, E.; Mann, D.; Kim, W.; Lu, Y. R. *Nano* **2006**, *1*, 1.
- (8) Burke, P. J. *Solid State Electron.* **2004**, *48*, 1981.
- (9) Zhong, Z.; Gabor, N. M.; Sharping, J. E.; Gaeta, A. L.; McEuen, P. L. *Nat. Nanotechnol.* **2008**, *3*, 201.
- (10) Krishnan, A.; Dujardin, E.; Ebbesen, T. W.; Yianilos, P. N.; Treacy, M. M. J. *Phys. Rev. B* **1998**, *58*, 14013.
- (11) Kis, A.; Zettl, A. *Philos. Trans. R. Soc. London, Ser. A* **2008**, *366*, 1591.
- (12) Cleland, A. N., *Foundations of Nanomechanics*; Springer-Verlag: Berlin, 2003.
- (13) Sapmaz, S.; Blanter, Y. M.; Gurevich, L.; van der Zant, H. S. J. *Phys. Rev. B* **2003**, *67*, 235414.
- (14) Sazonova, V.; Yaish, Y.; Ustunel, H.; Roundy, D.; Arias, T. A.; McEuen, P. L. *Nature* **2004**, *431*, 284.
- (15) Ustunel, H.; Roundy, D.; Arias, T. A. *Nano Lett.* **2005**, *5*, 523.
- (16) Peng, H. B.; Chang, C. W.; Aloni, S.; Yuzvinsky, T. D.; Zettl, A. *Phys. Rev. Lett.* **2006**, *97*, No. 087203.
- (17) Witkamp, B.; Poot, M.; van der Zant, H. S. J. *Nano Lett.* **2006**, *6*, 2904.
- (18) Chiu, H. Y.; Hung, P.; Postma, H. W. C.; Bockrath, M. *Nano Lett.* **2008**, *8*, 4342.
- (19) Lassagne, B.; Garcia-Sanchez, D.; Aguasca, A.; Bachtold, A. *Nano Lett.* **2008**, *8*, 3735.
- (20) Freitag, M.; Martin, Y.; Misewich, J. A.; Martel, R.; Avouris, P. *Nano Lett.* **2003**, *3*, 1067.
- (21) O'Connell, M. J.; Bachilo, S. M.; Huffman, C. B.; Moore, V. C.; Strano, M. S.; Haroz, E. H.; Rialon, K. L.; Boul, P. J.; Noon, W. H.; Kittrell, C.; Ma, J. P.; Hauge, R. H.; Weisman, R. B.; Smalley, R. E. *Science* **2002**, *297*, 593.
- (22) Misewich, J. A.; Martel, R.; Avouris, P.; Tsang, J. C.; Heinze, S.; Tersoff, J. *Science* **2003**, *300*, 783.
- (23) Chen, J.; Perebeinos, V.; Freitag, M.; Tsang, J.; Fu, Q.; Liu, J.; Avouris, P. *Science* **2005**, *310*, 1171.



- (24) Avouris, P.; Chen, J. *Mater. Today* **2006**, *9*, 46.
- (25) Bosnick, K.; Gabor, N.; McEuen, P. *Appl. Phys. Lett.* **2006**, *89*, 163121.
- (26) Lee, J. U.; Gipp, P. P.; Heller, C. M. *Appl. Phys. Lett.* **2004**, *85*, 145.
- (27) Zhou, Y. X.; Gaur, A.; Hur, S. H.; Kocabas, C.; Meitl, M. A.; Shim, M.; Rogers, J. A. *Nano Lett.* **2004**, *4*, 2031.
- (28) Lee, J. U. *Appl. Phys. Lett.* **2005**, *87*, No. 073101.
- (29) Lee, J. U.; Codella, P. J.; Pietrzykowski, M. *Appl. Phys. Lett.* **2007**, *90*, No. 053103.
- (30) Marty, L.; Adam, E.; Albert, L.; Doyon, R.; Menard, D.; Martel, R. *Phys. Rev. Lett.* **2006**, *96*, 136803.
- (31) Gabor, N. M.; Zhong, Z.; Bosnick, K.; Park, J.; McEuen, P. L. *Science* **2009**, *325*, 1367.
- (32) Kong, J.; Soh, H. T.; Cassell, A. M.; Quate, C. F.; Dai, H. J. *Nature* **1998**, *395*, 878.
- (33) Franklin, N. R.; Wang, Q.; Tomblor, T. W.; Javey, A.; Shim, M.; Dai, H. J. *Appl. Phys. Lett.* **2002**, *81*913.
- (34) Hines, D. R.; Mezhenny, S.; Breban, M.; Williams, E. D.; Ballarotto, V. W.; Esen, G.; Southard, A.; Fuhrer, M. S. *Appl. Phys. Lett.* **2005**, *86*, 163101.
- (35) Sangwan, V. K.; Ballarotto, V. W.; Fuhrer, M. S.; Williams, E. D. *Appl. Phys. Lett.* **2008**, *93*, 113112.
- (36) Zhang, Y. Y.; Zhang, Y.; Xian, X. J.; Zhang, J.; Liu, Z. F. *J. Phys. Chem. C* **2008**, *112*, 3849.
- (37) Here, ON/OFF ratio is limited by the dynamic range of our measurement setup.
- (38) Typical annealings are carried out at 250 °C in helium for 5 min for Pd and at 400 °C for Au. No annealing is necessary for freshly deposited metal electrodes .
- (39) Sazonova, V. A Tunable Carbon Nanotube Resonator. PhD. Thesis, Cornell University, Ithaca, NY 2006.